Proceedings of the
International Conference on Mechanical Engineering and Renewable Energy 2011
(ICMERE2011) 22- 24 December 2011, Chittagong, Bangladesh

ICMERE2011-PI-199

FLOW AND PERFORMANCE SIMULATIONS OF WIND POWER UNIT

Yuta Usui[1*], Toshiaki Kanemoto[2] and Koichi Kubo[1, 3]

[1]Graduate School of Engineering, Kyushu Institute of Technology, Sensui 1-1, Tobata, Kitakyushu, Fukuoka, Japan
[2]Faculty of Engineering, Kyushu Institute of Technology, Sensui 1-1, Tobata, Kitakyushu, Fukuoka, Japan
[3]JSPS Research Fellow
k344108y@tobata.isc.kyutech.ac.jp[*], Kanemoto@mech.kyutech.ac.jp, h584104k@tobata.isc.kyutech.ac.jp

Abstract-The authors have invented the superior wind power unit composed of the tandem wind rotors and the double rotational armature type generator without the traditional stator. The large-sized front wind rotor and the small-sized rear wind rotor drive the inner and the outer armatures respectively, in keeping the rotational torque counter-balanced. Such operating conditions may be able to make the output higher than the traditional wind turbines, and to keep the output constant in the rated operation mode without the brakes and/or the pitch control mechanisms. This paper discusses numerically the flow conditions around the single wind rotor as the first step to simulate the flow condition around the tandem wind rotors. The simulated results of output characteristics and the velocity distribution are almost the same as the experimental results. Such comparisons suggest that the flow conditions around the tandem wind rotors may be predicted by the numerical simulation.

Keywords: Wind Turbine, Wind Energy, Tandem Wind Rotors, Numerical Analysis, Flow condition

1. INTRODUCTION

Wind is clean, renewable and homegrown energy source of the electric power generation, and has been positively/effectively utilized to cope with the warming global environment. The traditional wind turbines, however, may have some weak points as follows. The large-sized wind rotor generates the high output at the moderate wind velocity, but it is not operated at the weak wind in general. The small-sized wind rotor is suitable for the weak wind, but the output is smaller. That is, the size of the wind rotor must be correctly/appropriately selected in conformity with the wind circumstances. Moreover, the blade of the wind rotor must be equipped with the brakes and/or the pitch control mechanisms, in general, to suppress the abnormal rotation and generated overload at the strong wind, and to keep the good quality of the electric power supply. To overcome these weak points, the authors have invented the superior wind power unit [1], as shown in Fig. 1. This unit is composed of the large-sized front wind rotor, the small sized rear wind rotor and the peculiar generator with the inner and the outer armatures without the traditional stator. The front and the rear wind rotors for the upwind type drive the inner and the outer armature, respectively. The rotational speeds and the directions of both wind rotors/armatures are free, and automatically adjusted pretty well in response to the wind circumstances. Then, this unit is called "Intelligent Wind Power Unit" by the authors. The idea of the tandem wind rotors has been proposed [2], and the output has been increases more or

less [3]-[6] while providing the traditional generator with the gearbox. The proposed tandem wind rotors, however, are operated in cooperation with the double rotational armature type generator without the gearbox and the pitch control mechanism. The superior operation of this unit was verified in the previous papers [7]-[9].

To predict the flow conditions and the performances of the tandem wind rotors in Intelligent Wind Power Unit, this paper simulates the output and the flow conditions around the front wind rotor as the preliminary step.
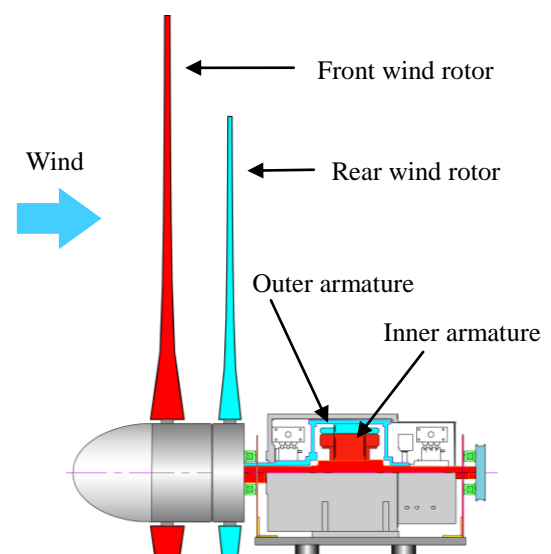

Fig.1 Intelligent Wind Power Unit (Upwind type)

2. SUPERIOR OPERARION OF TANDEM WIND ROTORS

The operation of the tandem wind rotors is in cooperation with the double rotational armature type generator, as shown in Fig. 2. The rotational directions and the speeds of tandem wind rotors/armatures are automatically adjusted in response to the wind speed, as described above. Both wind rotors start to rotate at the low wind speed, namely the cut-in wind speed, but the rear wind rotor counter-rotates against the front wind rotor. The rear wind rotor reaches the maximum rotational speed at the rated wind speed. With more increase of the wind speed, the rotational speed of the rear wind rotor decreases gradually, stops, and then begins to rotate in the same rotational direction as the front wind rotor, so as to coincide the rotational torques with that of the front wind rotor. Such behaviors are caused from that the small-sized wind rotor must work in the blowing mode against the attacking wind, because the rear wind rotor in the turbine mode cannot generate the same rotational torque as the large-sized front wind rotor. As a result, the operating conditions mentioned above enable successfully to guarantee the quality of the electric power in the rated operating mode without the traditional brakes and/or pitch control mechanisms. Moreover, the counter-rotation makes the output higher even at poor wind circumstances, which is a remarkable advantage for the area having unacceptable wind circumstance to the power generation.

3. MUMERICAL SIMULATION METHOD AND MODEL WIND ROTOR

The flow conditions around the wind rotor were simulated by the commercial CFD code of ANSYS-CFX ver.12 with SST turbulent model at the steady state conditions. Figure 3 shows the domains of the flow simulation with the grids generation. These domains have tetra grids, and have prism grids on the blade surface in order to simulate accurately the flow in the boundary layer (see Fig. 4). Domains of the flow simulation are separated into the rotating domain close to the wind rotor and the stationary domain surrounding the rotating domain, and these domains were connected with the velocity and the pressure. The grid number is about 9,000,000 for the rotating domain and about 700,000 for the stationary domain. At the inlet boundary, the wind velocity V was given at the wind tunnel nozzle of the diameter 800 mm which is set in front of the wind rotor. The flow can cross the boundaries surrounding the domains, but leave at the outer boundaries of stationary domain. These flows given as the boundary condition are uniform at the specified cross section.

In order to compare the numerical simulation with the experimental result, the geometry of the model wind rotor was same as one of experiment. The diameter of the front wind rotor is $d_F = 500$ mm. The blade profiles are shown in Fig. 5, namely Front Blade G in the previous paper [9], where the blade is formed with MEL002 aerofoil [10] and has the twist to get the desirable angle of attack irrespective of the radial position, respectively. The front blade setting angle, measured from the tangential direction at the tip (see
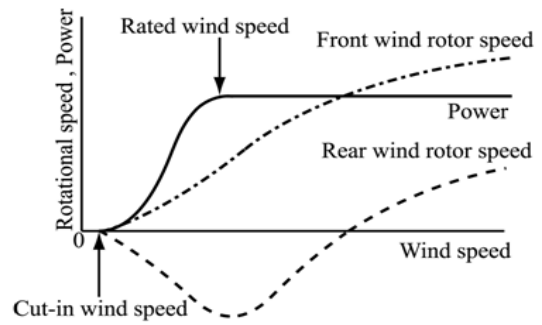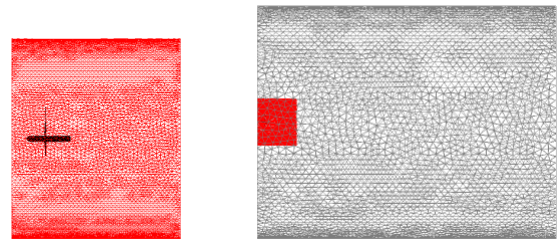

Fig.2 Operation of Intelligent Wind Power Unit

(a) Rotating domain   (b) Stationary domain

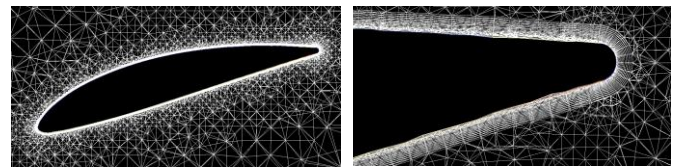Fig.3 Domains of the flow simulation with grid generation
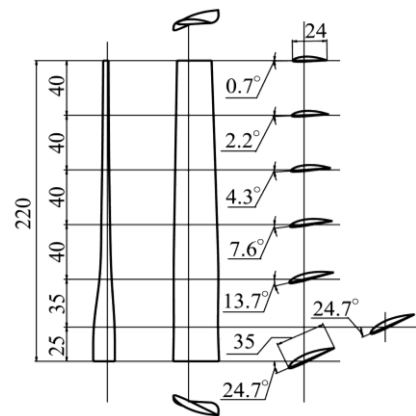

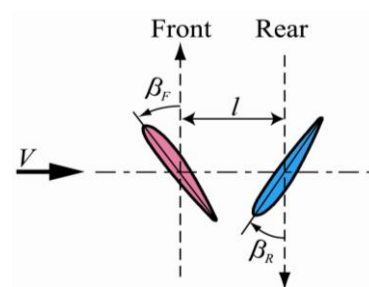Fig.4 Prism grid on the blade

Fig.5 Front Blade G

Fig.6 Blade setting angles

Fig.6), are $\beta_F = 0$ degrees. The blade number is $Z_F = 3$. These dimensions are optimized in the previous paper[9].

4. SIMULATION OF SINGLE WINE ROTOR

In order to evaluate the reliability of the numerical simulation, the output and the flow condition of the front wind rotor (without the rear wind rotor) are simulated and compared with the experimental results.

4.1 Output

Figure 7 shows the output coefficient against the tip speed ratio, where C_P is the output coefficient [$C_P = P$ /
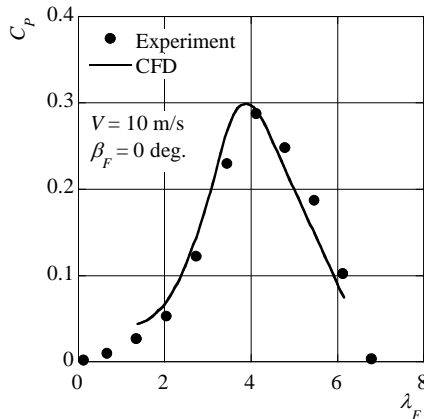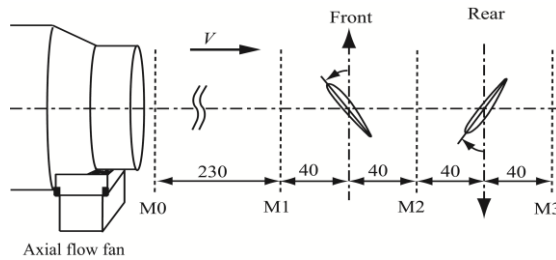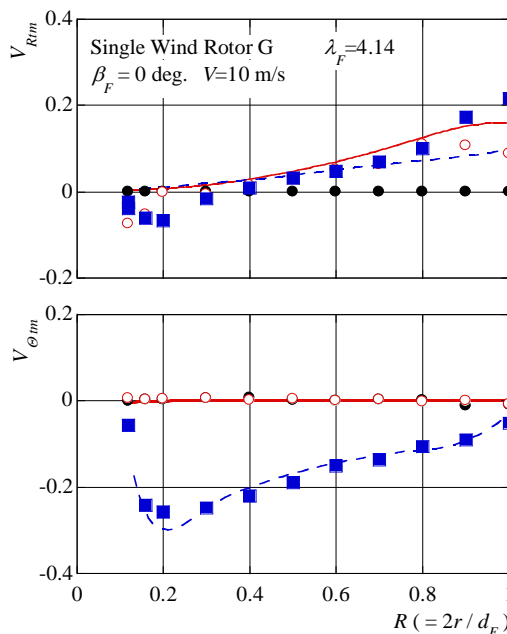
Fig.7 Output of the single wind rotor

Fig.8 Positions of the measurement sections

$(\rho A V^3 / 2)$, ρ: density, $A = \pi d_F^2 / 4$, V: wind velocity, P: output] and λ_F is the tip speed ratio [λ_F = (the tip speed of the front wind rotor) / V]. The simulated results given in curves give close agreement with the experiments, and the maximum output is at about $\lambda_F = 4$.

4.2 Flow Condition at the Maximum Output

The flow condition around the front wind rotor was simulated numerically at the maximum output operation ($\lambda_F = 4.14$), where the measurement sections are shown in Fig. 8. Figure 9 shows the velocity and the angle of attack distributions averaged in the tangential direction at each radius, where V_{Mtm}, $V_{\Theta tm}$ and V_{Rtm} are the axial, the swirling (positive in the rotational direction) and the radial velocity (positive in the outward direction) components divided by the inlet wind velocity V at Section M0, and R is the dimensionless radius divided by the front wind rotor radius (= $d_F / 2$). The angle of attack α_F was estimated with the flow conditions at Section M1 and the blade setting angle at each radius position. The simulated velocities and the angle of attack distributions agree well with the experimental results which were measured by the 5 holes pitot tube quantitatively. The velocity has the radial component V_{Rtm} and the axial velocity component V_{Mtm} decreases even at Section M1 due to the blockage effect, namely the drag force. Moreover, the numerical simulation can also predict obviously the more decrease of the axial velocity at Section M2, especially close to the blade tip. The front wind rotor discharges the swirling flow as recognized Section M2.

4.3 Effect of Tip Speed Ratio on Flow Condition

Figure 10 shows the velocity components at $\lambda_F = 2.46$ and 6.07 separated from $\lambda_F = 4.14$ giving the maximum output (see Fig. 9). The radial velocity component V_{Rtm} increases at the blade tip with the increase of the tip speed ratio. That is, the blockage effect, namely the drag force, of the wind rotor may increase with the increase of the rotational speed. Such a drag force affects the axial velocity component which decreases with the increase of the rotational speed. Besides, the swirling velocity
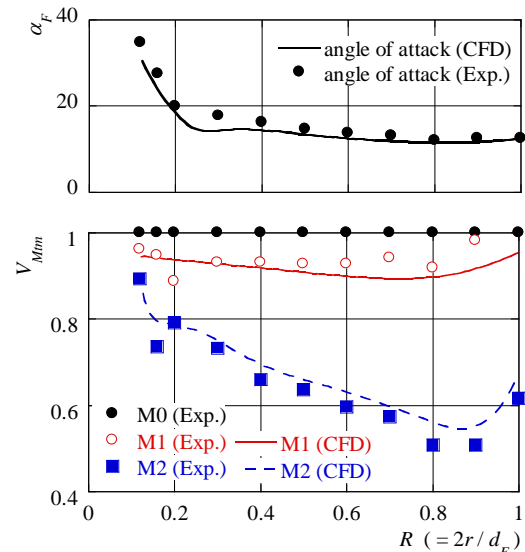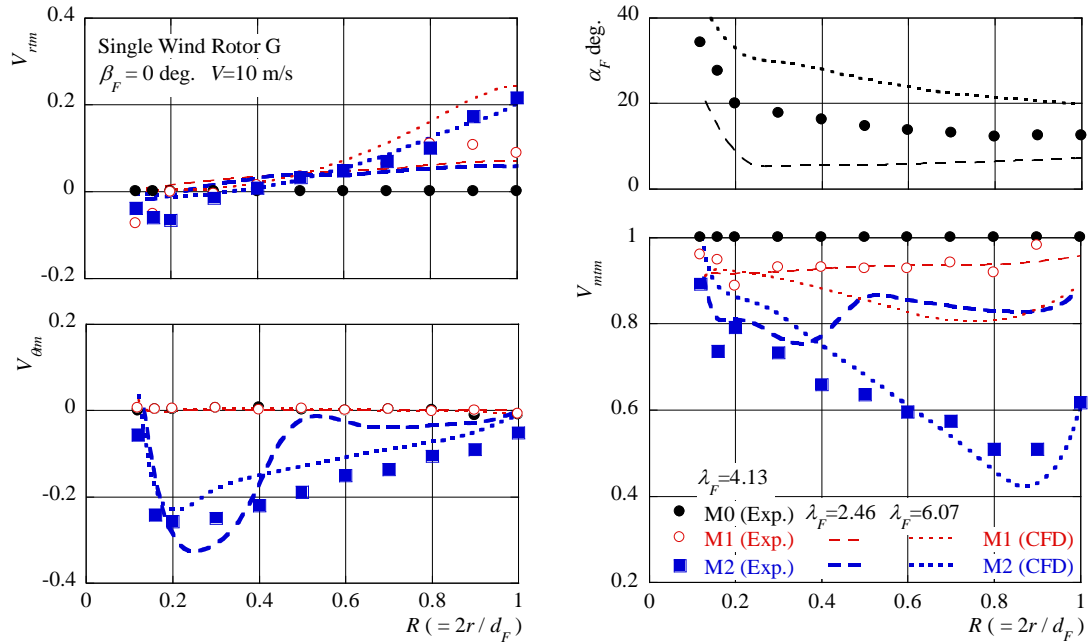
Fig.9 Flow conditions around the single wind rotor

Fig.10 Effect of the tip speed ratio on the flow conditions

component $V_{\Theta tm}$ affects the output C_P, and C_P at $\lambda_F = 2.46$ having the faster $V_{\Theta tm}$ is higher than one at $\lambda_F = 6.07$ (see Fig. 7). These results may be derived from the characteristics of MEL002 aerofoil [10].

5. FLOW AROUND TANDEM WIND ROTORS

As the above simulation method is effective to predict the output and the flow conditions around the single wind rotor, the method was provided for the tandem wind rotors in this chapter. The tandem wind rotors composed of front wind rotor presented above and Rear Blades G given in Fig. 11, where the blade number of the rear wind rotor is $Z_R = 5$ and the rotational diameter is $d_R = 210$ mm. The front and the rear blade setting angles are $\beta_F = 5$ degrees and $\beta_R = 15$ degrees. The dimensionless axial distance between the front and rear wind rotor twist centers is L [$= l / d_F$, l: the axial distance] $= 0.16$. These dimensions are also optimized in the previous paper [9].

In the simulation, the grid generation is the same as one in the single wind rotor, and the rotating domain was separated into front wind rotor domain and the rear wind rotor domain. These domains were connected by Frozen Rotor Interface to take the flow interactions into consideration, as shown Fig. 12.

Figure 13 shows the velocity and the angle of attack distributions in the radial direction, where the angle of attack α_R for the rear blade is estimated with the flow conditions at Section M2 and the rear blade setting angle. The swirling velocity component at the smaller radius of Section M3 is much larger than the experimental result, but the component scarcely contributes to generate the rotational torque because of the smaller radius. The rotational torque is controlled by the flow condition at the larger radius and the conditions agree well with the experimental results.

Above results suggest that the flow condition around the tandem wind rotors may also be able to be predicted by the numerical simulation.

6. CONCLUDING REMARKS

The output and the flow condition of the single wind rotor were simulated numerically at the various rotational speeds, and the results are in good agreement with the experiments. The simulation was also provided for the tandem wind rotors, and has the acceptable results in comparison with the experimental results.

Authors will optimize the blade profiles by the numerical simulation to not only improve the output but also reduce the acoustic noise.
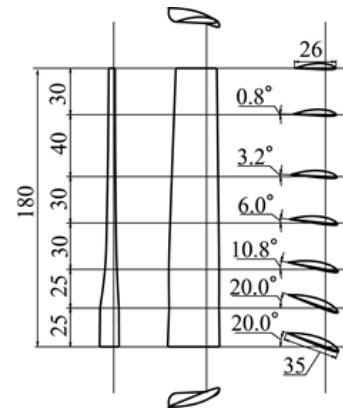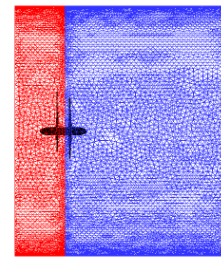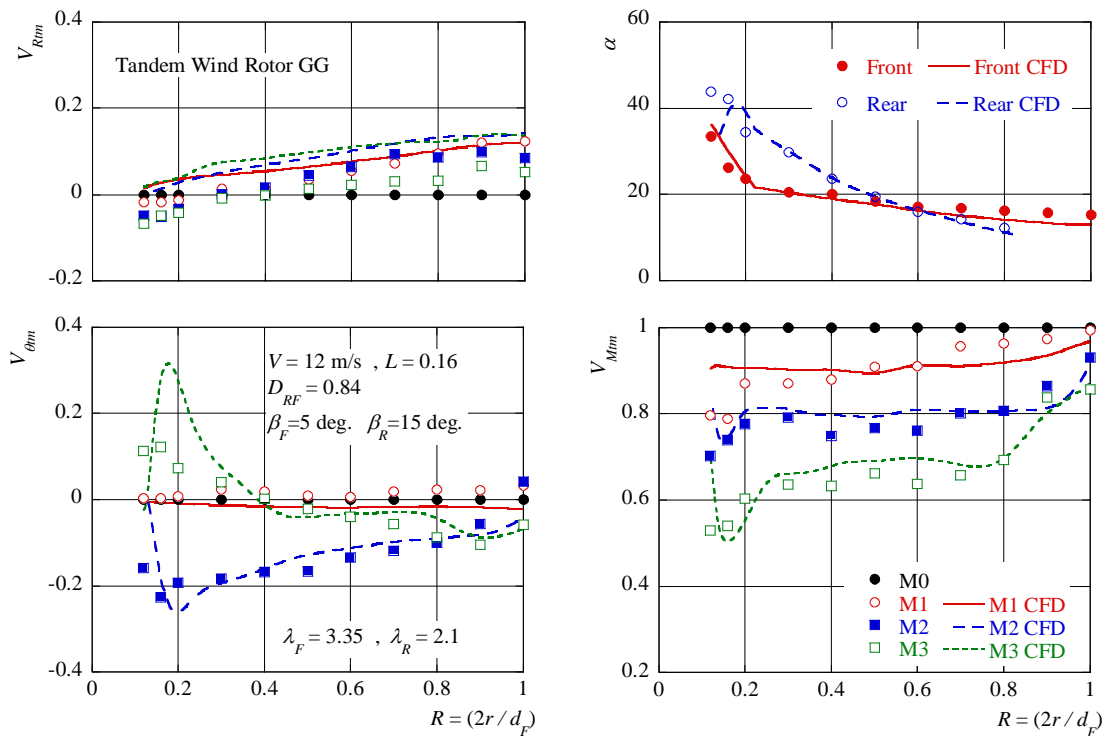

Fig.11 Rear Blade G

Fig.12 Rotating domains

Fig.13 Flow conditions around the tandem wind rotors

8. REFERENCES

[1] T. Kanemoto, et al., "Intelligent Wind Turbine Generator with Tandem Rotors Applicable to Offshore Wind Farm*"*, *Proceedings of the 15th International Offshore and Polar Engineering Conference and Exhibition*, Seoul, Korea, 2005.

[2] David A. Spera, *Wind Turbine Technology*, ASME Press, 1994, p.93.

[3] K. Appa, "Counter rotating wind turbine system", *Energy Innovations Small Grant (EISG) Program Technical Report*, 2002.

[4] K. Kubo, N. Mihara, A. Enishi, and T. Kanemoto, "Acoustic Noise from Tandem Wind Rotors of Intelligent Wind Power Unit" *Journal of Thermal Science*, Vol.19, No.2, pp.120-125, 2010.

[5] S.N. Jung, T.S. No, and K.W. Ryu, "Aerodynamic performance prediction of 30kW counter-rotating wind turbine system", *Renewable Energy*, Vol.30, No.5, pp.631-644, 2005.

[6] http://www.kowintec.com/english/intro/info.htm. (Sep. 9, 2011)

[7] T. Kanemoto, and A.M. Galal, "Development of Intelligent Wind Turbine Generator with Tandem Wind Rotors and Double Rotational Armatures", *ISME International Journal*, Ser. B, vol. 49, no.2, pp.450-457, 2006.

[8] T. Kanemoto, et al., "Intelligent wind turbine generator with tandem rotors applicable to offshore wind form (characteristics of the peculiar generator and the performance of three dimensional blades)", *Proceeding of the 17th International offshore and polar engineering conference*, Lisbon, Portugal, 2007, pp.363-368.

[9] K. Kubo, and T. Kanemoto, "Development of Intelligent Wind Turbine Unit with Tandem Wind Rotors and Double Rotational Armatures (2nd Report, Characteristics of tandem wind rotors)", *Journal of Fluid Science and Technology*, Vol.3, No.3, pp.370-378, 2008.

[10] http://riodb.ibase.aist.go.jp/db060/index.html. (Sep. 20, 2011)